

# The effect of substrate surface roughness on the wettability of Sn-Bi solders

YI-YU CHEN, JENQ-GONG DUH\*

*Department of Materials Science and Engineering, National Tsing Hua University, Hsinchu, Taiwan*

*E-mail: jgd@mse.nthu.edu.tw*

BI-SHIOU CHIOU

*Department of Electronic Engineering, National Chiao Tung University, Hsinchu, Taiwan*

The effect of substrate surface roughness on the wettability of Sn-Bi solders is investigated by the eutectic Sn-Bi alloy on Cu/Al<sub>2</sub>O<sub>3</sub> substrates at 190 °C. To engineer the surface with different roughnesses, the Cu-side of the substrates is polished with sandpaper with abrasive number 100, 240, 400, 600, 800, 1200, and 1 μm alumina powder, respectively. Both dynamic and static contact angles of the solder drops are studied by the real-time image in a dynamic contact angle analyzer system (FTA200). During dynamic wetting, the wetting velocity of the solder drop decreases for the rougher surface. However, the time to reach the static contact angle seems to be identical with different substrate surface roughness. The wetting tip of the solder cap exhibits a waveform on the rough surface, indicating that the liquid drop tends to flow along the valley. As the solder drops reach a static state, the static contact angle increases with the substrate surface roughness. This demonstrates that the wettability of solders degrades as the substrates become rough.

## 1. Introduction

Soldering technology plays an important role in current SMT high-density electronic packages. In the soldering process, a solder joint is made by bringing molten solder into contact with a metal surface with which the solder forms a bond. Thus, the wettability between solders and substrates is a critical reliability issue because it is the crux of joint formation. The driving force of liquid solders wetting on substrates is mainly the interfacial energies and the interfacial reactions [1, 2]. Besides, the substrate surface roughness might alter the interfacial energy and the wetting mechanism as the solder drop contacts the substrate and thus influences both the static and dynamic contact angles [3–5].

Early modeling carried out by Wenzel [6] to discuss the effect of surface roughness on wetting has a thermodynamic approach in which the additional surface area produced by roughening the substrate was regarded as effectively causing an increase in its surface energy. This implies that the apparent contact angle decreases with the roughness ratio if the contact angle is less than 90°. However, a different prediction by Shuttleworth and Bailey [7] pointed out that rough surfaces cause the contact line to distort locally, which gives rise to a spectrum of micro-contact angles near the solid surface and the apparent contact angle increases with the surface roughness. This discrepancy of the models between Wenzel and Shuttleworth was resolved by regarding the asperities as a series of energy barriers that must be overcome as the liquid front spreads over the surface [8–

10]. It was also noted that Wenzel behavior was found in very well-wetting system [11]. Recently, Zhou and De Hosson [12] argued that rough grooves can be categorized into two types, i.e., radial and circular grooves in the middle of which a liquid drop is placed. Any type of grooves on a practical rough surface is a combination of these two types of grooves.

To meet the requirement of environmental concern, unleaded solders have been developed to replace the conventional Pb-Sn solder [13–16]. Recently, microstructure evolution and mechanical testing of the unleaded solder joints were conducted in our research group [17, 18]. The purpose of this study is to investigate the wetting behavior of an unleaded Sn-Bi solder on the Cu metallized Al<sub>2</sub>O<sub>3</sub> substrate. The effect of substrate roughness of the metallized substrate will be investigated by examining the static and dynamic wettability.

## 2. Experimental procedure

The thick-film Cu/Al<sub>2</sub>O<sub>3</sub> substrates were supplied by ERSO (Electronic Research Service Organization, Taiwan), and cut by a diamond saw into 1 cm × 1 cm pieces. The thickness of Cu conductors was measured to be about 15 μm. The Cu-sides of the substrates were first polished with sandpaper with abrasive number of 100, 240, 400, 600, 800, and 1200, along with 1 μm alumina powder, respectively, and then cleaned ultrasonically in acetone and alcohol for 10 min. Fig. 1 shows the schematic diagram of the polished Cu substrate. For

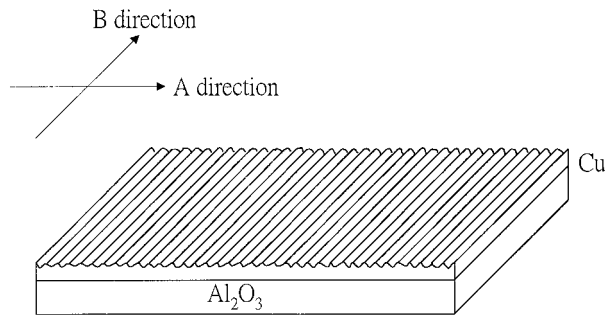


Figure 1 Schematic diagram of the polished Cu substrate.

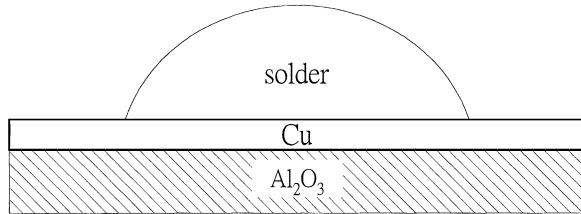


Figure 2 Solder drop on the Cu/Al<sub>2</sub>O<sub>3</sub> assembly.

convenience, the axes of the valleys will be referred to as the B direction and their normal as the A direction. The surface roughness,  $R_a$ , and wavelength,  $\lambda_a$ , of the substrates in the A direction were measured by an  $\alpha$ -step (Alpha-Step 250, Tencor Instruments, USA).

The eutectic Sn-Bi solder alloy was fabricated from raw materials including pure tin and pure bismuth (purity > 99.9%, Chung-Cheng Inc., Taiwan). They were then diced into small pieces and placed on the Cu/Al<sub>2</sub>O<sub>3</sub> substrates of different surface roughness. The solder/Cu/Al<sub>2</sub>O<sub>3</sub> assembly was then placed in the dynamic contact

angle analyzer system (FTA200, Firsttenangstroms, USA), mingled with RMA flux and then melted at 190 °C for reflowing to form a solder cap as indicated in Fig. 2.

The dynamic contact angle analyzer system was further used to measure the static and dynamic contact angles of solder drops. The measurement system is shown in Fig. 3. A camera system captures the *in situ* pictures of the solder drop. From the shape of the drop in the pictures, the static and dynamic contact angles can be measured.

### 3. Results and discussion

The results of surface roughness and wavelength of the substrates in the A direction with different abrasive number are summarized in Table I. The values of the measured surface roughness are close to those in the literature [19]. From the models proposed by Shuttleworth and Bailey [7], the contact angle in the rough surface must consider the steepness  $\alpha_m$ , which is the angle of the local surface, by an expression of the type

$$\theta_r = \theta_0 \pm \alpha_m \quad (1)$$

where  $\theta_r$ ,  $\theta_0$ , and  $\alpha_m$  are illustrated in Fig. 4. The steepness can be measured by the root mean square (RMS) surface high,  $R_a$ , and the average distance between surface asperities,  $\lambda_a$ , by the expression

$$\alpha_m = \tan^{-1} K(R_a/\lambda_a) \quad (2)$$

where  $K$  is the arithmetic factor,  $R_a/\lambda_a$  is a measure of the RMS surface slope. Fig. 5 shows the value  $R_a/\lambda_a$

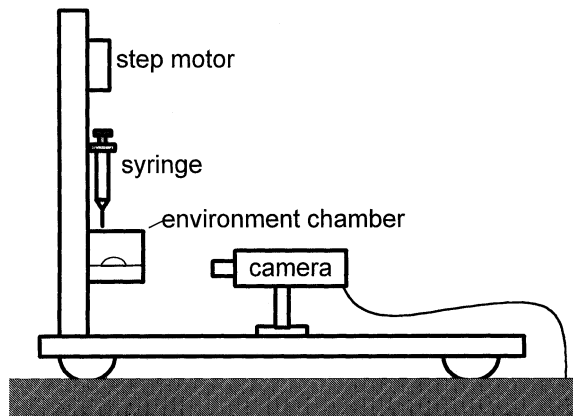


Figure 3 Schematic diagram of the dynamic contact angle analyzer system.

TABLE I Surface roughness and wavelength of the substrates in the A direction with different abrasive number

Abrasive number	Surface roughness, $R_a$ ( $\mu\text{m}$ )	Wavelength $\lambda_a$ ( $\mu\text{m}$ )
100	$1.81 \pm 0.14$	16.4
240	$0.80 \pm 0.03$	7.75
400	$0.49 \pm 0.03$	7.25
600	$0.19 \pm 0.01$	5.25
800	$0.11 \pm 0.01$	—
1200	$0.10 \pm 0.01$	4.5
1 $\mu\text{m}$ alumina powder	$0.05 \pm 0.01$	—

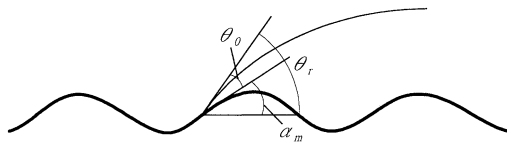


Figure 4 Schematic illustration of the surface features of the drop resting on a rough surface.

with different abrasive number. It indicates that the value  $R_a/\lambda_a$  increases inversely with the abrasive number.

The eutectic Sn-Bi solder was reflowed at 190 °C for 5 min. Fig. 6 show the top view of the wetting tip of the eutectic Sn-Bi solder on the Cu substrates with the abrasive number 100 as it was cooled down to room temperature. The wetting tip of the solder cap exhibits a waveform and its wavelength is about 10  $\mu\text{m}$ , indicating that the liquid drop prefers to flow along the valley. The effect of surface roughness on wetting in the eutectic Sn-Bi/Cu system is shown in Fig. 7.  $\theta_A$  and  $\theta_B$  are static contact angles in the A direction and B direction, respectively, after 5 min reflowing. The result shows that both  $\theta_A$  and  $\theta_B$  increase progressively as the roughness increases. The top view of the drop looks like an oval shape, and the schematic diagram can be illustrated in Fig. 8. The drop diameters parallel to the abrasive direction of the substrate ( $R_B$ ) are always longer than the perpendicular one ( $R_A$ ). Fig. 9 shows the variation of the ratio  $R_A$  to  $R_B$  with different surface roughness. It indicates that the ratio remains a constant at about 0.9 as the surface roughness increases. According to the models proposed by Dettre *et al.* [6], asperities are regarded as a series of energy barriers that must be overcome as the liquid front spreads over the surface. The ability of a liquid to overcome such barriers and spread depends on the relative sizes of its vibrational energy and the barrier. In this study, the liquid front moving in the A direction must overcome the energy barriers of the valleys. Moving along the B direction has a lower energy barrier because of the spreading of the liquid over the grooves. This renders the drop oval in shape.

Wetting phenomena in the solder/Cu system are complex because of the formation of intermetallic compounds. Besides the consideration of interfacial energy and viscosity, the formation energy of interfacial reactions between the liquid solder and the metal

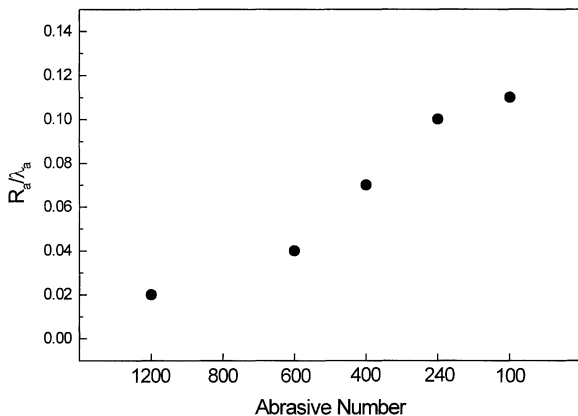


Figure 5  $R_a/\lambda_a$  as a function of different abrasive numbers.

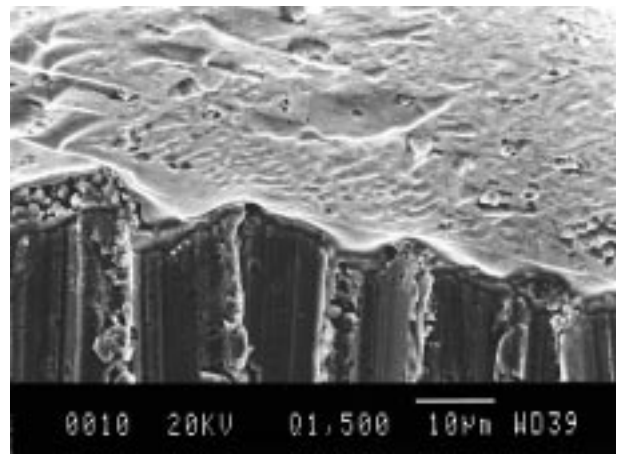


Figure 6 Top view of wetting tip of the eutectic Sn-Bi solder on Cu with the abrasive number 100.

substrate plays an important role in the driving force of the wetting. On the basis of theoretical models by Shuttleworth and Bailey, as mentioned previously, there is a local contact angle existing at the point of the triple line on the rough surface. The wetting process is influenced by this local distortion. In the reactive wetting systems, the wetting process is driven not only by surface tension but also by the reactive energy. Thus, wetting on rough surfaces involves both factors. If the reactive energy only is considered, a rough surface has more active sites over the nominal unit area. The reaction will be more intensive and the wetting tends to progress. Theoretically, the contact angle on the rough surface will be decreased. On the other hand, if the surface morphology and the local contact angle on the wetting tip are only focused, the result may be opposite. In Fig. 8, the contact angle increases with surface roughness. This reveals that the effect of surface geometry is dominant as the eutectic Sn-Bi solder wets on a rough substrate. The contact angle hysteresis is enhanced with a rough surface and the contact angle will not be reduced if the energy of compound formation does not overcome the barriers of the hysteresis. In Fig. 8, the reaction may be more intensive on the rough surface, although the geometry of the rough surface and the contact angle hysteresis cause the wetting to decrease with the surface roughness.

During the wetting process, dynamic wetting is another important and critical issue that needs to be

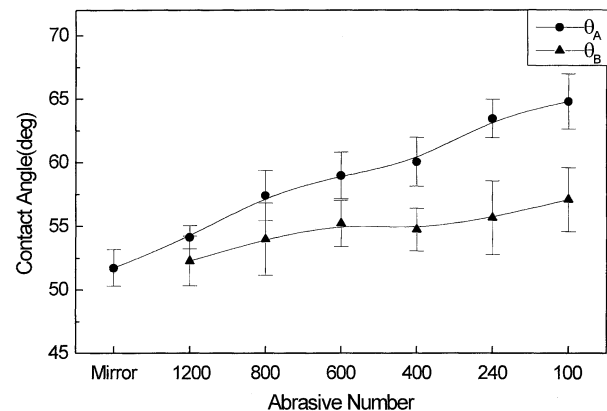


Figure 7 Static contact angle  $\theta_A$  and  $\theta_B$  of eutectic Sn-Bi solder on Cu substrates with different surface roughness.

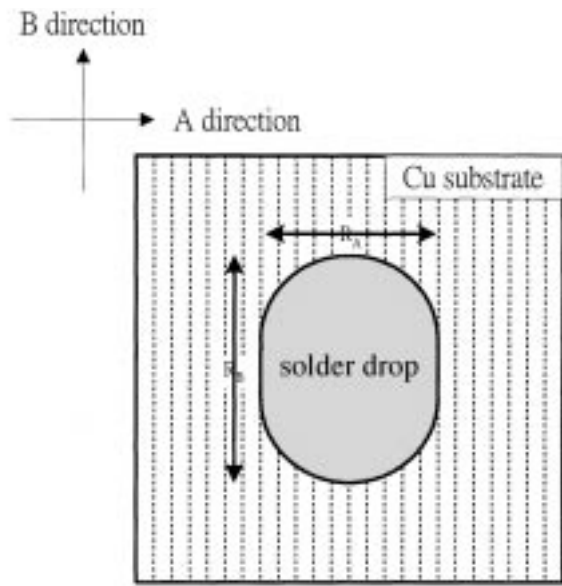


Figure 8 Top view of the solder drop on the Cu substrate.

discussed. The measurement of the dynamic wetting of the eutectic Sn-Bi solder were also carried out at 190 °C on Cu substrates of different roughness, as shown in Fig. 10. The contact angles degrade as an exponential decay and reach a steady state in the final stage. The slopes of these curves are nearly identical in the initial stage, yet deviate after 50 s. It appears that the contact angles reach a steady state after 125 s reflowing.

For normal liquids, the effect of gravity on drop shape can be neglected if the drop is small, and the shape of the drop will approximate a spherical cap. The velocity of the wetting line can be given by [20]

$$v = \frac{\partial r}{\partial t} = - \frac{\partial \theta}{\partial t} \left( \frac{3V}{\pi} \right)^{1/3} \frac{(1 - \cos \theta)^2}{(2 - 3 \cos \theta + \cos^3 \theta)^{4/3}} \quad (3)$$

Where  $V$  is the volume of the drop,  $r$  is the base radius, and  $\theta$  is the instantaneous dynamic contact angle. Fig. 11 represents the velocity of contact line of solder drop wetting on Cu substrates with different surface roughness, and Fig. 12 is its corresponding value with different substrate surface roughness after 20 s and 50 s reflowing.

The velocity decays to zero as the dynamic wetting

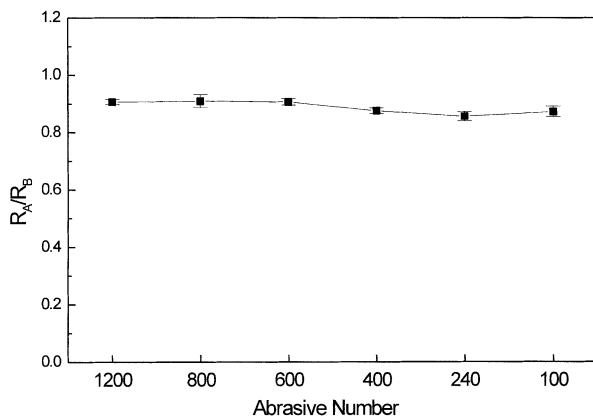


Figure 9 Ratio of drop diameter  $R_A$  and  $R_B$  of water wetting on Cu substrates with different surface roughness.

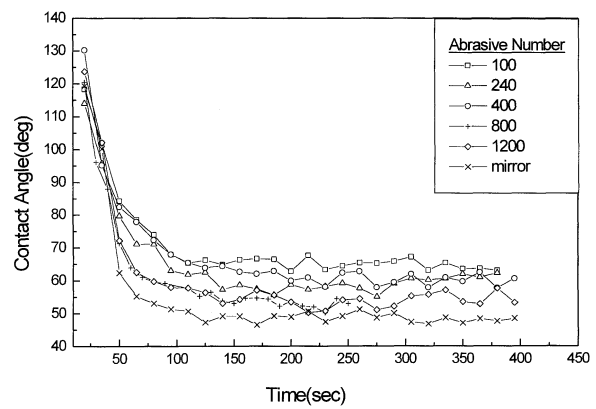


Figure 10 Dynamic contact angle of the eutectic Sn-Bi solder on Cu substrates with different surface roughness at 190 °C.

achieves a steady state. Dynamic wetting on the rough surface behaves differently as compared to the smooth surface. The velocity on the smooth surfaces is higher than that on the rough surfaces. However, the time to reach the static contact angle seems to be the same with different substrate surface roughness.

The effect of surface roughness on dynamic wetting is not well known yet. Cazabat and Cohen Stuart [5] studied the effect of surface roughness on dynamic contact angle in the systems of “completely wetting”, which means that the static contact angle is close to zero. It was found that the liquid spreading on the rough surface has some similarities with wetting of porous bodies. The wetting velocity on the rough surface is higher than that in the smooth surface. It is close to the combination of the diffusion and the capillarity mechanism. However, in the partial wetting system, the contact angle of the liquids is usually smaller than 90°, yet not close to zero. The liquid does not perceive the roughness and behaves as if the surface is smooth, and the diffusion mechanism fails to prevail. Besides the variation between completely and partial wetting, the discrepancy of the wetting phenomenon for the eutectic SnBi/Cu systems from the wetting model as proposed by Cazabat and Cohen Stuart may be also attributed to both the driving force of wetting and the viscosity of liquids. In addition, the influence of contact angle hysteresis during dynamic wetting must also be considered. The friction of wetting increases with the

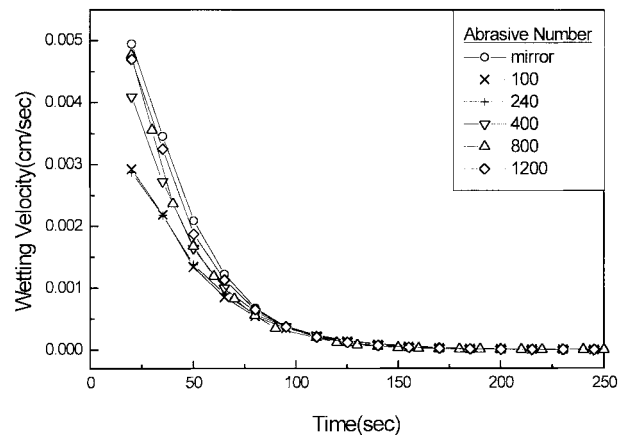


Figure 11 Wetting velocity of the eutectic Sn-Bi solder on Cu substrates with different roughness at 190 °C.

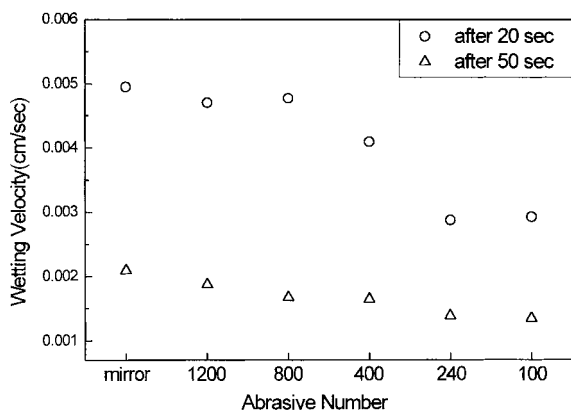


Figure 12 Wetting velocity of the solder cap with different substrate surface roughness after 20 s and 50 s reflowing.

surface roughness, which causes the contact angle hysteresis. Consequently, the mobility of the contact line is impeded, and the velocity of the wetting tip is slower on the rough surface.

The soldering process in microelectronic packaging requires good wettability between solders and substrates. In the eutectic SnBi/Cu system, with the wetting velocity decreases and the static contact angle increases with the surface roughness. These imply that the wettability will be degraded if the substrate is too rough. The smoother surface is required if the wetting properties are ameliorated in the electronic package. In addition to the wettability of solders, the mechanical properties of solder joints, such as fracture toughness or fatigue life, are also influenced by the surface roughness of substrates [19,21]. In general, the rough surface has a positive effect, but sometimes a negative one. In fact, more theoretical models are required and the selection of the roughness of the substrate must depend on the functionalities of interest.

#### 4. Conclusion

In this study, the effect of substrate surface roughness on the wettability of solders is investigated by the eutectic Sn-Bi solder soldering on Cu/Al<sub>2</sub>O<sub>3</sub> substrates at 190 °C. A measurement technique is developed to investigate the wettability of solders on the metallized substrate in the consideration of both static and dynamic wetting. It is argued that the surface energy and thus the wetting mechanism of the solder are dependent on the surface roughness of the substrate, which in turn reflects variation in both the static and dynamic contact angles.

During dynamic wetting, the wetting velocity of the solder drop decreases on the rough surface. However, the time to reach the static contact angle appears similar despite substrate surface roughness. As the solder drops reach a static state, the static contact angle increases with the substrate surface roughness. It is demonstrated that the wettability of solders degrades as the substrates become rough.

#### Acknowledgments

The authors acknowledge financial support from the National Science Council, Taiwan, under contracts No. NSC 86-2221-E007-043 and NSC 87-2218-E-007-024.

#### References

1. X. H. WANG and H. CONDRAD, *Metall. Mater. Trans. A* **26A** (1995) 459.
2. H. K. KIM, H. K. LIOU and K. N. TU, *J. Mater. Res.* **10** (1995) 497.
3. X. B. ZHOU and J. TH. M. DE HOSSON, *ibid.* **10** (1995) 1984.
4. S. J. HITCHCOCK, N. T. CARROLL and M. G. NICHOLAS, *J. Mater. Sci.* **16** (1981) 714.
5. A. M. CAZABAT and M. A. COHEN STUART, *J. Phys. Chem.* **90** (1986) 5845.
6. R. N. WENZEL, *Ind. Eng. Chem.* **28** (1936) 988.
7. R. SHUTTLEWORTH and G. L. J. BAILEY, *Disc. Faraday Soc.* **3** (1948) 16.
8. R. H. DETTRE and R. E. JOHNSON, *Ave. Chem. Ser.* **43** (1963) 112.
9. C. HUH and S. G. MASON, *J. Colloid Interface Sci.* **60** (1977) 11.
10. J. D. EIK and R. J. GOOD, *ibid.* **53** (1975) 235.
11. M. G. NICHOLAS and R. M. CRISPIN, *J. Mater. Sci.* **21** (1986) 522.
12. X. B. ZHOU and J. TH. M. DE HOSSON, *J. Mater. Res.* **10** (1995) 1984.
13. J. GLAZER, *Int. Mater. Rev.* **40** (1995) 65.
14. E. P. WOOD and K. L. NIMMO, *J. Electron. Mater.* **23** (1994) 709.
15. P. G. HARRIS and M. A. WHITMORE, *Circuit World* **19** (1993) 25.
16. M. MCCORMACK and S. JIN, *J. Electron. Mater.* **23** (1994) 635.
17. Y. Y. WEI and J. G. DUH, *J. Mater. Sci., Mater. Electron.* **9** (1998) 373.
18. Y. G. LEE and J. G. DUH, *ibid.* **10** (1999) 33.
19. E. I. STROMSWOLD, R. E. PRATT and D. J. QUESNEL, *J. Electron. Mater.* **23** (1994) 1047.
20. M. J. DE RUIJTER and J. DE CONINCK, *Langmuir* **13** (1997) 7293.
21. D. YAO and J. K. SHANG, *IEEE Trans. Compon. Packaging, Manuf. Technol. Part B* **19** (1996) 154.

Received 22 November 1999  
and accepted 3 February 2000